Carcinogenesis vol.35 no.5 pp.983–991, 2014
doi:10.1093/carcin/bgt393
Advance Access publication December 3, 2013

CHIP/Stub1 functions as a tumor suppressor and represses NF-κB-mediated signaling in colorectal cancer

Yangmeng Wang, Fangli Ren, Yinyin Wang, Yarui Feng, Dianjun Wang[1], Baoqing Jia[1], Ying Qiu, Shiyan Wang[2], Jun Yu[2], Joseph JY Sung[2], Jiake Xu[3], Nikolajs Zeps[4,5] and Zhijie Chang*

State Key Laboratory of Biomembrane and Membrane Biotechnology, School of Medicine, National Engineering Laboratory for Anti-tumor Therapeutics, Tsinghua University, Beijing 100084, China, [1]Departments of General Surgery and Pathology, Chinese PLA General Hospital, Beijing 100853, China, [2]Institute of Digestive Disease and Department of Medicine & Therapeutics, Li KaShing Institute of Health Sciences, CUHK Shenzhen Research Institute, The Chinese University of Hong Kong, Hong Kong, China, [3]School of Pathology and Laboratory Medicine, The University of Western Australia (M504), Crawley WA 6009, Australia, [4]Colorectal Cancer Research Unit, The University of Western Australia (M509), Crawley WA 6009, Australia and [5]St John of God HealthCare, The Bendat Family Comprehensive Cancer Centre, Subiaco WA 6008, Australia

*To whom correspondence should be addressed. Tel: +86 10 62785076; Fax: +86 10 62773624;
Email: zhijiec@tsinghua.edu.cn

The carboxyl terminus of Hsc70-interacting protein (CHIP, also named Stub1), a U-box containing E3 ubiquitin ligase, is involved in degradation of certain oncogenic proteins. Recent studies indicated that CHIP suppresses tumor progression in human cancers by targeting Src-3, hypoxia inducible factor 1α, NF-κB, ErbB2 and c-Myc. Here, we report that CHIP was downregulated, predominantly, in the late stages of human colorectal cancer (CRC), and that the *CHIP* promoter was hypermethylated in CRC specimens. Overexpression of CHIP in HCT-116 cells resulted in impaired tumor growth in nude mice and decreased abilities of tumor cell migration and invasion. Conversely, depletion of CHIP in HCT-116 cells promoted tumor growth and increased tumor cell migration and invasion. CHIP was further found to negatively regulate NF-κB signaling in HCT-116 cells by promoting ubiquitination and degradation of p65, a subunit of the NF-κB complex. The suppressive effect of CHIP led to decreased expression of NF-κB-targeted oncogenes including *Cyclin D1, c-Myc, MMP-2, VEGF* and *IL-8*. We proposed that CHIP inhibits the malignancy of CRC cells, possibly through targeting NF-κB signaling. This study provides functional evidence for CHIP as a potential tumor suppressor in CRC, and CHIP expression may be a marker for stages of CRC.

Introduction

Colorectal cancer (CRC) is one of the most common cancers in the world with a high mortality rate. Advanced therapeutic techniques and increased availability of new cytotoxic drugs have improved the outcome of CRC patients, but 50% of patients still die from the metastatic disease (1). Abnormal genetic and epigenetic alterations in several signaling pathways are responsible for multistep development of CRC through increasingly malignant stages to metastasis (2). Well-characterized events involved in CRC development have been characterized as inactivation of APC, p53 and PTEN; mutation of K-Ras; CpG island hypermethylation of tumor suppressor genes and abnormal activation of PI3K-AKT pathway. IL-6-STAT3 and NF-κB pathways are also constitutively activated and drive the expression of pro-oncogenic genes in CRCs, especially in the colitis-associated CRC (3).

Abbreviations: CHIP, carboxyl terminus of Hsc70-interacting protein; CRC, colorectal cancer; FBS, fetal bovine serum; shRNA, short hairpin RNA.

The carboxyl terminus of Hsc70-interacting protein (CHIP), also named Stub1, was identified as a co-chaperone protein and a U-box containing E3 ligase (4). CHIP has been shown to promote the ubiquitination and degradation of chaperone-bound proteins and misfolded proteins including CFTR (5), GR (6) and mutant SOD1 (7). We have demonstrated that CHIP mediated ubiquitination and degradation of Smads (8), Runx1 (9) and Runx2 (10) *in vitro*. More importantly, CHIP is also involved in degradation of several oncogenic proteins including ErbB2 (11), hypoxia inducible factor 1α (12), c-Myc (13), Runx1 (9), estrogen receptor α (14), Met receptor (15) and SRC-3 (16). Recent studies suggest that CHIP functions as a tumor suppressor and is downregulated in human breast cancer (targeting SRC-3) (16) and gastric cancer (targeting NF-κB p65) (17). To date, the role of CHIP in the development of CRC has not been explored.

In this study, we investigated the functional significance of CHIP in the development and metastasis of CRC and uncovered that CHIP suppresses CRC development through inhibiting NF-κB pathway by meditating ubiquitination and degradation of p65.

Materials and methods

Cell lines and CRC tissue samples

HCT-116 and LS180 cells were obtained from American Type Culture Collection and cultured in McCoy's 5A and minimum essential medium supplemented with 10% fetal bovine serum (FBS) and 1% penicillin/streptomycin. HCT-116 stable cell lines of CHIP overexpression and depletion were screened by G418 (700 μg/ml) from cells transfected with pEFneo-HA-CHIP, pSilencer-CHIP short hairpin RNA (shRNA) (CHIP shRNA: 5′-GGACGACATCCCCAGCGCTCT-3′) and the control plasmids pEFneo-HA and pSilencer-Scramble. Stable pools of HCT-116 cells with neomycin resistance were used in this study.

CRC tissue microarrays were obtained from the Colorectal Cancer Research Unit, The University of Western Australia based at St John of God HealthCare, Subiaco with ethics approval granted by the St John of God HealthCare Human Research Ethics Committee. Human colon cancer tissues were obtained from 301 Hospital, Beijing, China. All samples used in the study were approved by the Ethical Committees in Chinese PLA General Hospital, The Chinese University of Hong Kong and The University of Western Australia, under the guidance of tissue collection procedure with informed consent.

Immunohistochemistry

The tissue microarray slides were incubated in a dry oven at 60°C for 1 h, then dewaxed in xylene for 3 × 30 min and rehydrated in 100%, 100%, 95%, 90%, 80% and 70% ethanol for 5 min each. Antigen retrieval was performed in a pressure cooker containing citrate buffer (0.01 M, pH 6.0) for 3 min. Endogenous peroxidase activity of the tissues was quenched by 3% H_2O_2 for 10 min. The slides were incubated with 10% goat serum for 30 min at 37°C, followed by incubation with primary CHIP polyclonal antibody overnight at 4°C. Biotin-labeled secondary antibody was applied to the slides and then the slides were incubated with streptavidin–peroxidase. Samples were developed using 3,3′-diaminobenzidine as substrates and further counterstained with hematoxylin.

An index of staining was used to indicate CHIP expression levels in colorectal cancer. The staining index was classified into four grades (negative = 0, weak = 1; moderate = 2, strong = 3) by the pathologists. Compared with normal tissue, if the staining index of tumor tissue is increased (T > N), CHIP expression is defined as 'high' in tumor tissue; if the staining index of tumor tissue is unchanged (T = N), CHIP level is defined as 'unchanged' and if the staining index of tumor tissue is decreased (T < N), CHIP level is designated as 'low' in colorectal cancer. TNM stage classification was defined as suggested by the American Joint Committee on Cancer and the International Federation of Gynecology and Obstetrics. In brief, T indicates the tumor size or direct extent of the primary tumor; N indicates nearby lymph node spread and M indicates presence of distant metatstasis.

Western blot and immunoprecipitation

Proteins extracted from cultured cells or tumor tissues were analyzed by western blot (18). For immunoprecipitation, HCT-116 cells were transfected with the indicated expression plasmids. After 48 h, cells were

lysed in lysis buffer (20 mM Tris–Cl, pH 7.4, 150 mM NaCl, 1 mM ethylene diamine tetra-acetic acid, 1% Triton X-100, 1 mM NaVO3, 2.5 mM sodium pyrophosphate, 1 mM β-glycerol phosphate, 1 mM phenylmethylsulfonyl fluoride, 5 μg/ml aprotinin, and 5 μg/ml leupeptin, pH 7.5). Appropriate antibodies (2 μg) and 30 μl protein G PLUS Agarose (Santa Cruz) beads were added to the cell lysates. The mixture was rotated at 4°C for about 4 h. The precipitated complexes and cell lysates were subjected to sodium dodecyl sulfate–polyacrylimide gel electrophoresis for western blot analyses.

Methylation-specific PCR

DNA methylation patterns in the CpG island of the *CHIP* promoter region were determined by methylation-specific PCR. Genomic DNA of CRC samples was extracted by using TIANamp Genomic DNA Kit (Tiangen Biotech, Beijing, China). Bisulfite modification of genomic DNA was performed by using the EZ DNA Methylation-Gold Kit (Zymo Research, Orange, CA). Primers used for methylation-specific PCR were previously reported (17): primers for methylated promoter region, 5′-AGTGAGGTATTTTATTGGGAAAGTC-3′ and 5′-GACGTCGAAAACT AAAAAAAACG-3′; primers for unmethylated promoter region, 5′-GTGAGGTATTTTATTGGGAAAGTTG-3′ and 5′-AACATCAAAAACT AAAAAAAACACT-3′. PCR was performed by using the AmpliTaq Gold DNA Polymerase system (Applied Biosystems, Foster City, CA), and the thermocycling conditions were an initial 5 min of denaturation at 94°C followed by 45 cycles (methylation-specific PCR) or 35 cycles (unmethylation-specific PCR) of 30 s at 94°C, 30 s at 50°C and 30 s at 72°C.

Methylated DNA immunoprecipitation

Human DNA Methylation Microarrays (Agilent Technologies) was used for analysis of DNA methylation in colon cancer. This array offers a more comprehensive set of DNA methylation regions including 27 627 expanded CpG islands and 5081 undermethylated regions. Briefly, purified genomic DNA extracted from HCT-116 and LS180, two normal colon tissues, was sheared by sonication. The sheared DNA fragments ranged in size from 200 to 500 base pairs. An aliquot (40 μl) of sheared DNA was set as the input DNA, which did not go through the immunoprecipitation process and was used as reference DNA. Methylated DNA was immunoprecipitated by anti-5-Methyl Cytidine antibody (ab10805, Abcam)/magnetic bead mixture and extracted by phenol–chloroform method together with reference DNA. The purified DNA was differentially labeled with fluorescent-labeled nucleotides by the Agilent Genomic DNA Enzymatic Labeling Kit. The reference DNA was labeled in the green channel (Cyanine 3) and the immunoprecipitated DNA was labeled in the red channel (Cyanine 5). The labeled DNA then was hybridized to their synthetic complementary DNA attached on the microarray slide, leaving its fluorescent tag. The fluorescent intensity was measured by a scanner for each spot on the microarray slide. The methylation values for each gene in each sample was represented as the log2 signal ratio of the immunoprecipitated DNA signal divided by the input control signal [log2 (IP/input)]. The relative methylation levels (defined as fold change) of each gene in HCT-116 and LS180 cells were normalized to the average log ratio in the two normal controls.

MTT assay

Tumor cell growth was examined by MTT assay (19). HCT-116 stable cell lines were seeded on 96-well plates at a density of 3000 cells/well with five repeats. At different time point, 5 mg/ml of MTT was added 4 h before termination of cell growth. The purple-blue sediment was dissolved in 150 μl of dimethylsulfoxide before harvest. The absorbance at 570 nm was measured with WELLSCAN MK3 ELIASA (Lab systems, Dragon, Finland) using a 630 nm reference filter.

Anchorage-independent growth in soft agar

Soft agar assay was performed as described (20). Briefly, 8×10^3 of cells were inoculated in 0.3% agar containing McCoy's 5A medium and seeded in each well of six-well plate containing 0.7% agar with McCoy's 5A medium. Cells were grown at 37°C for 21 days and stained with crystal violet (0.1% wt/vol) overnight. Colonies with diameter greater than 100 μm were counted.

Xenograft tumor model

HCT-116 cells (2×10^6, 100 μl) were subcutaneously inoculated in the flanks of BALB/c-nu/nu mice (6 weeks old). Seven mice were used in each group. Tumor volumes were monitored every 3 days and calculated using the following formula: volume = (length × width^2)/2. After 35 days, the mice were sacrificed, and the tumors were excised, applied to protein and RNA extraction or fixed for immunofluorescence staining. All the animal experiments were performed with the approval of the Scientific Investigation Board of Tsinghua University.

Migration and invasion assays

The *in vitro* wound healing assay was performed based on a reported protocol (21). Briefly, cells were seeded in six-well plates to generate a confluent monolayer. The monolayer was scratched with a sterile 200 μl pipette tip. Cells were treated with mitomycin for 30 min, then cultured in McCoy's 5A medium with 0.2% FBS. The wound scratches were photographed at 0 and 72 h after scraping. The sizes of the wound closure areas were analyzed by Image J.

Matrigel invasion assay was performed according to a previously reported protocol (22). The *in vitro* invasive abilities of the HCT-116 cell lines were evaluated using transwell chamber (Millipore Corp., Bedford, MA). A total of 5×10^4 cells in 250 μl McCoy's 5A medium were introduced into the upper chamber coated with 30 μl Matrigel (BD Biosciences, 1:5 diluted), and the medium with 10% FBS and 5 μg/ml Fibronectin (Sigma) was introduced into the lower chamber. Cells were allowed to invade the Matrigel for 72 h. The invaded cells were fixed in methanol and stained with 0.1% crystal violet (Sigma). The number of invaded cells per field was counted under a phase contrast microscope. Cells in five different fields of each well were counted and photographed.

Immunofluorescence

Paraffin-embedded xenograft tumors were sectioned to 5 μm. The sections were subjected to rehydration and antigen retrieval and blocked with 10% FBS. Then the sections were incubated with the CD31 antibody (sc-1506, Santa Cruz) overnight at 4°C. The primary antibody was detected by rabbit antigoat immunoglobin G/FITC secondary antibody. The nucleus was stained with 4′,6-diamidino-2-phenylindole. The sections were visualized with a confocal laser scanning microscope (OLYMPUS FV500).

Real-time PCR

Real-time PCR was performed to examine the expression of NF-κB target genes in HCT-116 cell lines. RNA was reverse transcribed using VigoScript First Strand complementary DNA Synthesis Kit (Vigorous Biotechnology), and the complementary DNA was subjected to real-time PCR analysis. Primer sequences are as follows: *GAPDH*: 5′-AACGT GTCAGTGGTGGACCTG-3′ and 5′-AGTGGGTGTCGCTG TTGAAGT-3′; *CyclinD1*: 5′-CCGAGAAGCTGTGCATCTACAC-3′ and 5′-AGGTTCCA CTTGAGCTTGTTCAC-3′; *c-Myc*: 5′-CAAACCTCCTCACAG CCCACT-3′ and 5′-TTCGCCTCTTGACATTCTCCTC-3′; *IL-6*: 5′-AAAGAGGCAC TGGCAGAAAA-3′ and 5′-TTTCACCAGGCAAGTCTCCT-3′; *IL-8*: 5′-GGTGCAGTTTTGCCAAGGAG-3′ and 5′-TTTCCTTGGGGTCCAG AC AG-3′; *MMP-2*: 5′-CGCTCAGATCCGTGGTGAG-3′ and 5′-TGTCACGTGG CGTCACAGT-3′; *VEGF*: 5′-AGTCCCATGAAGTGATCAAGTTCA-3′ and 5′-ATCCGCATGATCTGCATGG-3′;*CHIP*:5′-AGGCCAAGCACGACAAGT ACAT-3′ and 5′-CTGATCTTGCCACACAGGTAGT-3′. Real-time PCR was performed by using an SYBR Green master mixture on an HT7900 system (Applied Biosystems; Life Technologies).

Luciferase reporter assay

HCT-116 stable cell lines were seeded in 24-well plates, and cotransfected with pGL3-NF-κB luciferase reporter plasmid and renilla luciferase plasmid pRL-TK. Twenty-four hours later, cells were starved overnight and treated with or without 10 ng/ml tumor necrosis factor α for 8 h. Firefly and renilla luciferase activities were measured with the Dual-Luciferase Assay Kit (Vigorous Biotech Co., Beijing, China). Results were normalized by renilla luciferase luminescence intensity.

Statistical analysis

All experiments were repeated at least 3 times. Data are expressed as mean ± standard deviation. Significant differences between groups were determined using the Student's *t*-test. The χ^2 test was used for comparison of patient clinicopathologic characteristics. $P < 0.05$ was considered as statistically significant.

Results

CHIP expression is decreased in human CRCs

We first evaluated CHIP expression level in human CRC tissues. A western blot analysis with 35 cases of CRC samples demonstrated that CHIP expression was decreased in 48.6%, remained unchanged in 31.4% and increased in 20% of tumor specimens compared with adjacent non-tumor tissues (Figure 1A and B). A statistical analysis indicated that CHIP was significantly downregulated in the tumor tissues ($P < 0.01$) (Figure 1C). We further performed immunohistochemical staining experiments on tissue microarrays with 320 colorectal cancer

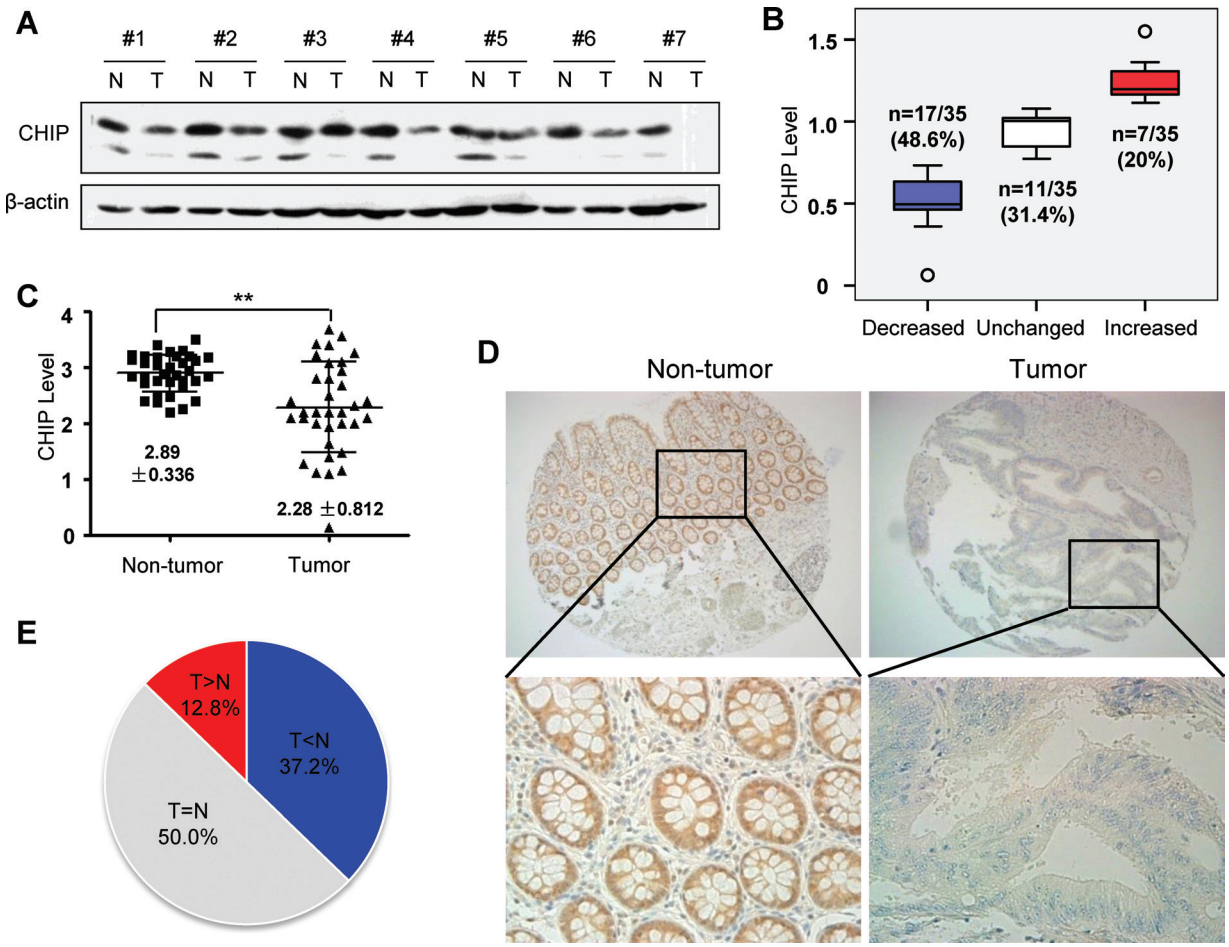

Fig. 1. CHIP expression is decreased in colorectal cancer. (**A**) Western blot analysis of CHIP proteins in seven representative patients. Paired normal (N) and tumor (T) tissues were subjected to a western blot analysis using polycolonal CHIP antibodies. (**B**) Difference of CHIP expression in tumors with CHIP downregulated (decreased), unchanged (unchanged) and upregulated (increased). CHIP expression level in tumor tissues was compared with the paired normal tissues. Band density of western blot was determined by Image J. A ratio of the quantified band density of CHIP in tumor tissue to that in the normal tissue was calculated. If the ratio was >1.1, CHIP level was defined as 'Increased'; if the ratio was between 0.75 and 1.1, CHIP level was 'Unchanged' and if the ratio was <0.75, CHIP level was 'Decreased'. (**C**) CHIP expression levels in non-tumor and tumor tissues of CRC samples. Samples of 35 patients were examined by western blot analyses. Band densities were calculated by Image J and normalized to β-actin levels. $^{**}P < 0.01$. (**D**) Representative images of immunohistochemistry staining of tissue microarrays using CHIP antibodies. The upper two images were photographed at 100-fold magnification, scale bar, 50 μm, and the lower images (×400) showed partial enlargement of the upper images. (**E**) A pie chart of the distribution of CHIP expression levels in tumor tissues compared with normal tissues on the tissue microarray. T > N: CHIP levels were increased in tumor tissues, T = N: CHIP levels were unchanged in tumor tissues, T < N: CHIP levels were decreased in tumor tissues. T, tumor tissue; N, normal tissue. The percentages of patients were shown. $P < 0.001$.

samples. Strong staining of CHIP in the normal tissue but weak in tumor is showen in Figure 1D. Statistically, we found that CHIP expression level in tumor tissues was decreased in 37.2%, remained unchanged in 50.0%, and increased in 12.8% of the samples in comparison with that in the normal tissues (Figure 1E). These results indicated that CHIP expression was frequently decreased in CRC.

To further reveal the role of CHIP on CRC, we performed an association study of CHIP expression in tumors with clinical features. The results showed that the expression level of CHIP was significantly associated with TNM stages ($P < 0.05$), a critical classification of malignant tumors, but not with age, gender or tumor site (Table I). Intriguingly, 31.7% of patients in stage I and II and 47.3% in stage III and IV showed decreased expression of CHIP (Table I). Overall, the correlation of CHIP expression and the TNM stages was −0.158 ($P < 0.05$). These results suggested that CHIP may regulate tumor development reflected by the TNM stage.

CHIP promoter is aberrantly methylated in human CRC

Downregulation of CHIP expression in human CRCs prompted us to examine whether hypermethylation occurs in the promoter regions of the *CHIP* gene as many tumor suppressor genes are often silenced by promoter hypermethylation during tumorigenesis and tumor progression. We performed a methylation-specific PCR to examine the methylation pattern of the *CHIP* promoter in 20 human CRC specimens from the 35 cases in Figure 1 (seven cases shown in Figure 2A and B). The corresponding CHIP expression levels are shown in Figure 1A. Our results indicated that considerably or totally methylated *CHIP* promoter was present in 45% (9 of 20) of the tumor tissues, whereas 75% (15 of 20) of the normal tissues were unmethylated or slightly methylated in the *CHIP* promoter in the 20 cases examined (Figure 2C). These results suggest that *CHIP* promoter is frequently hypermethylated in the CRC specimens. To further confirm whether CHIP hypermethylation occurs in CRC, we performed a methylated deoxyribonucleic acid (DNA) immunoprecipitation in CRC cells. We found that the promoter of *CHIP*, along with other frequently methylated promoters including *ZNF545*, *SOC2* and *BMP2*, was hypermethylated in CRC cells (HCT-116 and LS180) compared with normal tissues (increased by 1-fold, Figure 2D). Furthermore, a correlation study revealed that the decreased expression of CHIP correlated significantly to the hypermethylated *CHIP* promoter in tumor tissues in the same patients (Figure 2E). Therefore, hypermethylation of the *CHIP*

Table I. Association of CHIP expression in tumors with clinicopathologic features in 320 patients of colorectal cancers

Clinicopathological parameter	Total number of cases	CHIP expression			*P* value	*r*
		Decreased	Unchanged	Increased		
Age (year)						
≤65	110	44 (40.0%)	53 (48.2%)	13 (11.8%)	0.743	
>65	210	75 (35.7%)	107 (51.0%)	28 (13.3%)		
Gender						
Male	167	61 (36.5%)	91 (54.5%)	15 (9.0%)	0.066	
Female	153	58 (37.9%)	69 (45.1%)	26 (17.0%)		
Tumor site						
Proximal	157	60 (38.2%)	76 (48.4%)	21 (13.4%)	0.770	
Distal	145	54 (37.2%)	75 (51.7%)	16 (11.0%)		
TNM stage						
I and II	208	66 (31.7%)	111 (53.4%)	31 (14.9%)	0.013	–0.158*
III and IV	112	53 (47.3%)	49 (43.8%)	10 (8.9%)		

TNM stage: T, the size of the primary tumor and whether it has invaded nearby tissue; N, the amount of spread to nearby lymph nodes; M, distant metastasis.

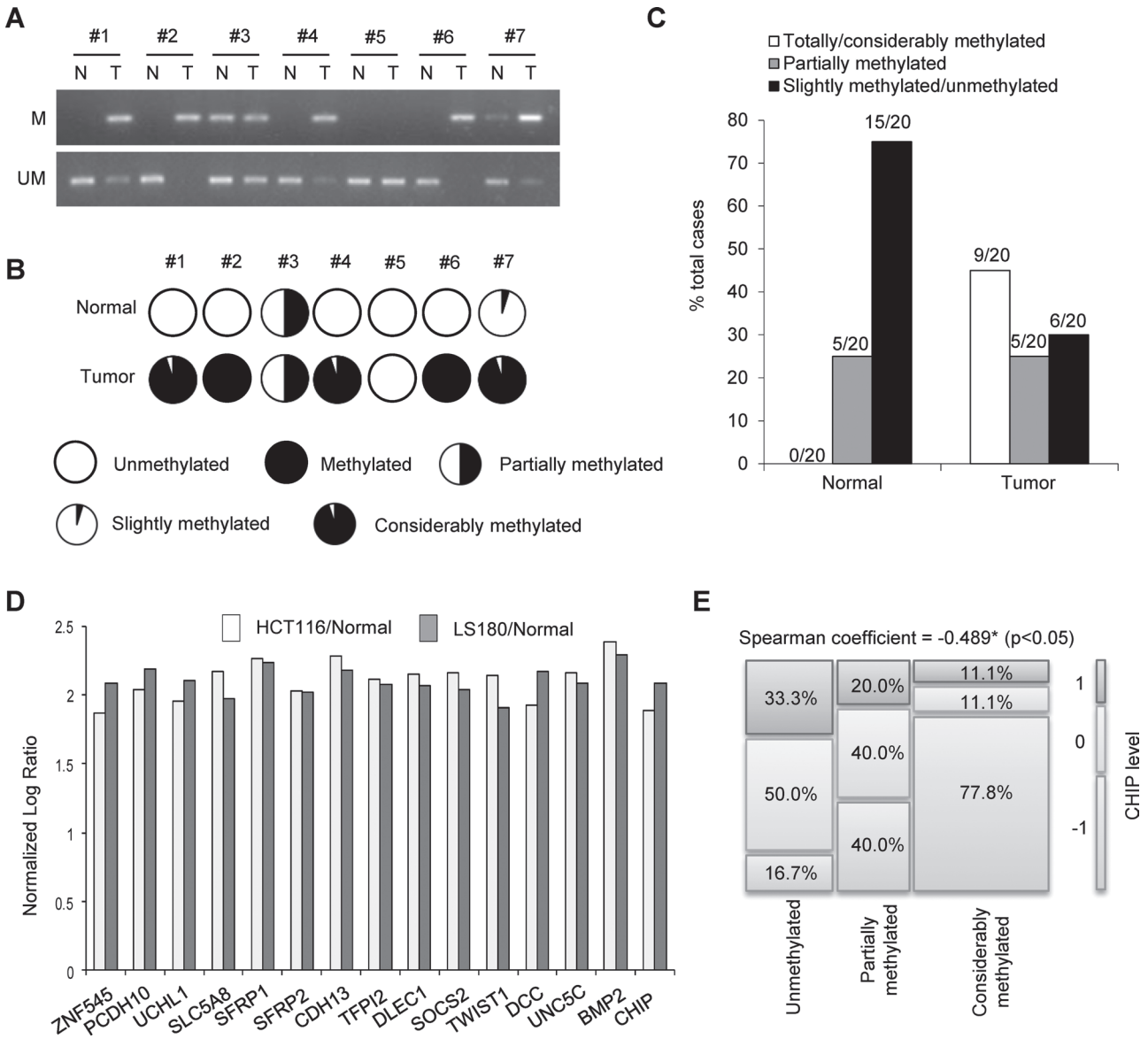

Fig. 2. *CHIP* promoter region is hypermethylated. (**A**) Detection of promoter methylation status of *CHIP* in CRC tumor tissues and paired non-tumor tissues by methylation-specific PCR ($n = 20$). Representative results were shown. (**B**) Methylation status of *CHIP* promoter region was presented by pie chart. N, normal tissue; T, tumor tissue. The seven cases were the corresponding cases shown in (A). (**C**) Distribution of different methylated status of *CHIP* promoter region in normal or tumor tissues. Percentages of patients with different levels of methylated *CHIP* promoter were calculated. (**D**) Hypermethylation of CHIP was detected along with the known tumor repressors in HCT-116 and LS180 cells. The methylation level of each gene promoter in HCT-116 or LS180 cells was normalized to that in the normal tissues. (**E**) Correlation of CHIP expression level and the promoter methylation status of CHIP in CRC tumor tissues.

promoter may provide a potential reason for the decreased CHIP expression level in colorectal tumor tissues.

CHIP suppresses CRC cell growth

The association of CHIP expression with the TNM stage prompted us to investigate the role of CHIP in CRC development. For this purpose, we generated stable cell lines overexpressing HA-CHIP or depleting CHIP by a small-interfering ribonucleic acid (RNA, assigned as CHIPi) in HCT-116 CRC cells (Figure 3A). We performed an MTT assay to examine the effect of CHIP on tumor cell growth *in vitro*. No significant changes of the cell numbers were observed in the CHIP-overexpressing or -depleted cells compared with the corresponding control cells (Figure 3B). Interestingly, CHIP-overexpressing cells formed fewer colonies than the control cells, but more colonies were observed by using CHIP-depleted cells in a soft agar colony formation assay (Figure 3C). Furthermore, we characterized the tumor formation ability of the cells in nude mice. The results showed that CHIP-overexpressing cells formed smaller tumors ($P < 0.01$), whereas, CHIP-depleted cells formed larger tumors in nude mice ($P < 0.01$; Figure 3D). Tumor growth curves illustrated faster growth of tumors formed by CHIP-depleted cells ($P < 0.01$) and slower growth by CHIP-overexpressing cells ($P < 0.01$; Figure 3E). A western blot analysis for the xenografts from different HCT-116 cells indicated the consistent maintenance of CHIP overexpression and depletion during the tumor formation in the nude mice (Figure 3F). Taken together, these data suggest that CHIP suppresses tumor growth of CRC cells.

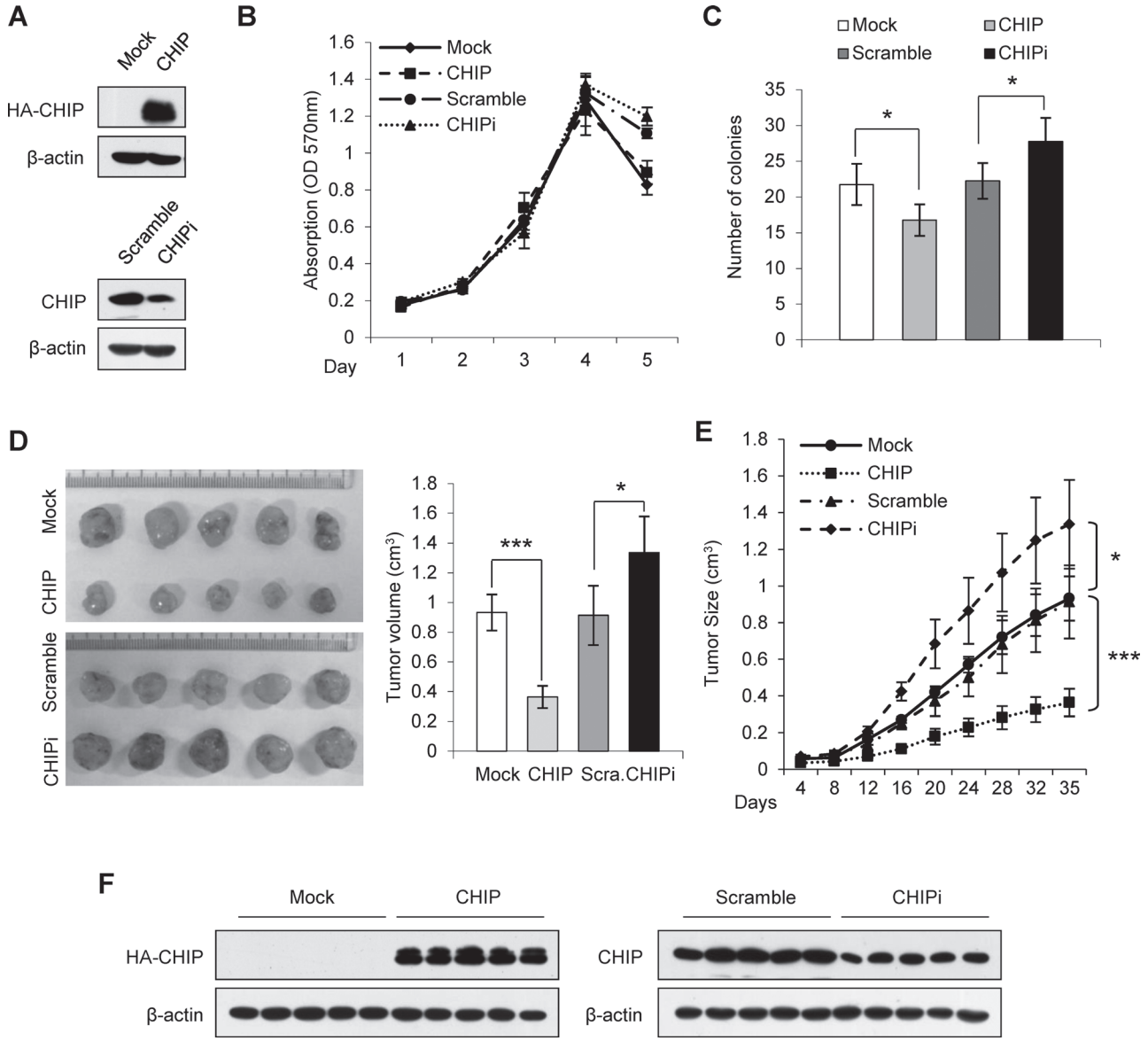

Fig. 3. CHIP suppresses CRC cell growth and colony formation. (**A**) Western blots showing the levels of HA-CHIP and endogenous CHIP in the stable overexpression (CHIP) and depletion (CHIPi) cell lines. (**B**) MTT assay of HCT-116 stable cell lines. A total of 3×10^3 of CHIP overexpression and depletion cell lines, together with the control cell lines, were seeded in 96-well plates. MTT assay was performed from day 1 to day 5. Data shown are mean ± standard deviation. (**C**) Colony formation assay of HCT-116 stable cell lines. A total of 8×10^3 of HCT-116 cell lines were seeded in six-well plates. After 21 days, colonies with diameter greater than 100 μm were counted in each well. Data are presented as mean ± standard deviation from three independent experiments. *$P < 0.05$. (**D** and **E**) Tumor formation experiment in nude mice. A total of 2×10^6 of HCT-116 stable cell lines were injected into the flanks of nude mice ($n = 5$). Tumor sizes were monitored during a period of 35 days. Tumor volume was calculated by the formula: volume = (length × width^2)/2. Xenografts of HCT-116 cell lines and the final tumor volumes were shown in (D), and tumor growth curves were shown in (E). Results shown are mean ± standard deviation. Scramble (Scra.) shRNA was used a control. *$P < 0.05$, ***$P < 0.001$. (**F**) Western blot analyses were performed to detect CHIP expression levels in the HCT-116 xenografts after sacrifice of the mice. HA-CHIP (left) and endogenous CHIP (right) were shown.

CHIP suppresses migration, invasion and angiogenesis abilities of CRC cells

To examine the effects of CHIP on the migration and invasion abilities of CRC cells, we performed *in vitro* wound healing and transwell assays. The result showed that CHIP-overexpressing cells migrated into the wound area much slower than the control cells (Figure 4A, top two panels), whereas CHIP-depleted cells experienced an accelerated migration (Figure 4A, bottom two panels). A quantitative analysis of the migration rates indicated that CHIP significantly inhibited CRC cell migration (Figure 4B). Transwell invasion assays showed that overexpression of CHIP decreased the invasion ability through matrigel-coated transwell chamber, whereas depletion of CHIP facilitated the cells to transmit the membrane (Figure 4C). Further quantitative analyses demonstrated that the invasive cell numbers of CHIP-overexpressing cells were significantly decreased than the control cells, whereas the invasive cell numbers were increased dramatically when CHIP was depleted (Figure 4D).

Since angiogenesis correlates with tumor growth and metastasis, we examined whether CHIP inhibits angiogenesis associated with growth of CRC cells in nude mice. We injected HCT-116 cells in nude mice and examined angiogenesis in the CRC xenografts by staining CD31, an endothelial cell marker. Tumor microvessel density was determined by counting the number of CD31 positive cells per mm^2. The results showed that microvessel density was decreased by 40% in the xenografts from the CHIP-overexpressing cells in comparison with the control xenografts, whereas it was increased when CHIP was depleted (Figure 4E). Quantitative analysis results indicated that the differences for microvessel formations in tumors formed by the CHIP-overexpressing or -depleted cells were statistically significant ($P < 0.005$ or $P < 0.05$; Figure 4F). All the results indicated that CHIP impairs the migration, invasion and angiogenesis ability of HCT-116 cells.

CHIP negatively regulating NF-κB pathway

Constitutive activation of NF-κB is involved in oncogenesis by regulating genes that promote tumor growth, angiogenesis and metastasis in human CRC (23). Based on our observations that CHIP suppressed tumor growth and metastasis of human CRCs, and a previous study that CHIP mediated degradation of NF-κB in gastric cancer (17), we questioned whether CHIP directly regulates NF-κB pathway in CRCs. A luciferase reporter assay showed that overexpression of CHIP repressed the NF-κB-driven luciferase activity in a dose-dependent manner (Figure 5A) and depletion of CHIP enhanced the NF-κB activity (Figure 5B) in HCT-116 cells. These results suggest that CHIP regulates the transcriptional activity of NF-κB. Indeed, qPCR analyses demonstrated an inverse relationship between CHIP expression and the expression of NF-κB-targeted genes (Figure 5C). In particular, genes targeted by NF-κB are those involved in tumor growth, angiogenesis and metastasis, including Cyclin D1, c-Myc, IL-8, MMP-2 and VEGF, which were downregulated in the CHIP-overexpressing cells but upregulated in the CHIP-depleted cells (Figure 5C). These results suggested that CHIP downregulated the NF-κB pathway in colorectal cancer cells.

CHIP functions as an E3 ubiquitin ligase of p65

To further investigate whether CHIP promotes degradation of the NF-κB complex in CRC cells, we examined the level of p65, a subunit of NF-κB, in HCT-116 cells transfected with increasing amounts of pEFneo-HA-CHIP plasmids. A western blot showed that the level of p65 was decreased with the increasing amounts of HA-CHIP proteins (Figure 5D, left three lanes). Interestingly, the level of p65 was restored when the cells were treated with MG132, a proteasome inhibitor (Figure 5D, right three lanes). To investigate whether CHIP mediates ubiquitination of p65, we performed an IP-Western experiment by precipitating p65 and examining ubiquitination. The results showed that CHIP dramatically promoted polyubiquitination of endogenous p65 proteins (upper panel, Figure 5E). These results suggested that CHIP mediates polyubiquitination and degradation of p65. Taken together, CHIP inhibits activation of NF-κB signaling by functioning as an E3 ubiquitin ligase for p65 in CRC.

Discussion

Clinical evidence has shown that upregulation of certain oncogenic proteins is caused by dysfunction of ubiquitin-mediated degradation process during tumorigenesis (24). Increasing number of E3 ubiquitin ligases have been found to be downregulated in a variety of human cancers. Several intensively studied E3 ubiquitin ligases, such as FBW7 (25–27), TRIM family (24), BRCA1 (28,29), VHL (30,31), FBXL2 (32,33) and Cul9 (34), were identified as tumor suppressors that target oncogene products. In this study, we found that CHIP was downregulated in CRCs and that promoter hypermethylation occurred in human colon tumors and CRC cell lines. Using clinical samples, we confirmed that CHIP was downregulated in most of the CRCs as examined by western blot and tissue array analyses. These two sets of results from different experiments were in close agreement in terms of the proportions of patients with CHIP downregulation and, importantly, we discovered that the level of CHIP expression was significantly associated with the TNM stage (Table I). In particular, the downregulation of CHIP expression was observed in more patients in advanced stage of tumors (Table I), suggesting that CHIP could be an important marker for tumor stages.

Tumor suppressors are always downregulated when hypermethylation occurs in their promoters. Our study provided evidence that *CHIP* promoter is hypermethylated in a large proportion of CRC patients. Although we observed that the expression of CHIP was highly corrected with the methylation status of *CHIP* promoter in the tumor tissues in most of the patients ($r = -0.489$, $P < 0.05$; Figure 2E), there remained 22.2% of patients with unchanged or increased CHIP expression (Figure 2E, last column). This finding implies that the hypermethylation occurred earlier than the protein level changes during tumorigenesis or CHIP expression could be regulated by other unknown factors. However, it is clear that the downregulation of CHIP in tumor patients was mainly caused by the methylation of its promoter, which resulted in inhibition of the transcription of CHIP. This is consistent with the fact that most of the E3 ubiquitin ligases including CHIP (16,17) are downregulated at the transcriptional level in cancers (24,26,30).

CHIP is a co-chaperone protein and possesses the E3 ubiquitin ligase activity (8). In this study, we found that CHIP targeted p65 and regulated the expression of NF-κB targeted genes. We have provided evidence that overexpression of CHIP inhibited and conversely that depletion of CHIP enhanced, the NF-κB signaling and changes in expression of several oncogenes including Cyclin D1, c-Myc, MMP-2, VEGF and IL-8. We revealed that CHIP promoted ubiquitination of p65 and this resulted in its degradation. We reasoned that downregulation of CHIP abolished its role in mediating the ubiquitination and degradation of p65, which further resulted in impaired NF-κB signaling. Since NF-κB plays an important role in controlling the tumor cell proliferation and migration, we concluded that downregulation of CHIP is an important component of tumorigenesis and CHIP could be an important factor that regulates NF-κB during tumorigenesis.

Decreased CHIP protein level in colon cancer may activate signaling pathways critical in 'hallmarks of the cancer' proposed by Hanahan and Weinburg (35). NF-κB signaling is an essential pathway involved in multistage of colon cancer development (36). This pathway affects tumor growth, angiogenesis and metastasis of CRC through inducing expression of important molecules that are involved in these events. We showed that CHIP suppressed NF-κB transcriptional activity, decreased messenger RNA levels of NF-κB target genes and regulated cell migration, invasion and angiogenesis abilities. Based on these findings, we proposed that the role of CHIP in inhibition of tumor growth, accompanied with impaired abilities of migration, invasion and angiogenesis, was dependent on the downregulation of NF-κB signaling.

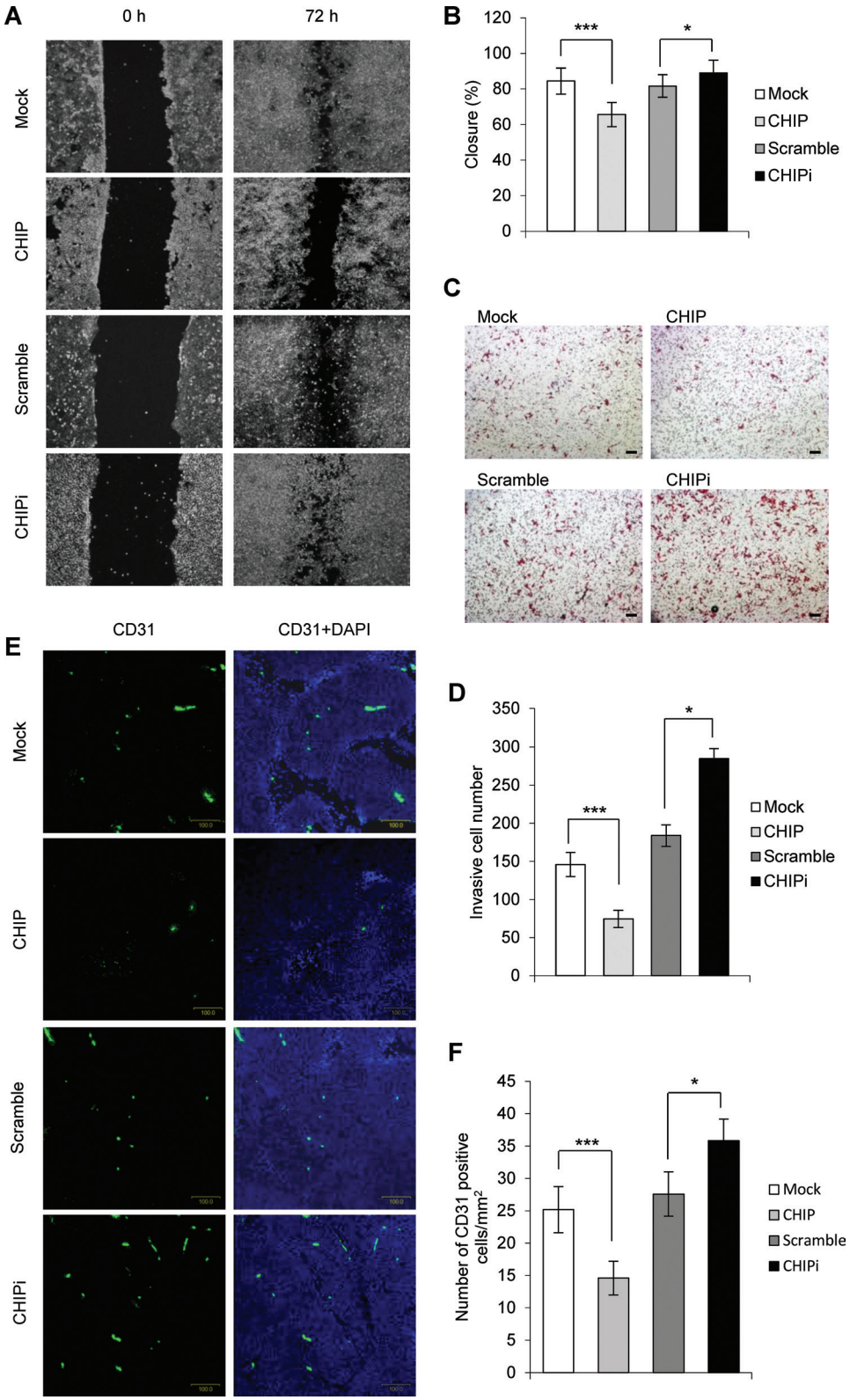

Fig. 4. CHIP suppresses migration, invasion and angiogenesis abilities of HCT-116 cells. (**A**) Wound healing assay of HCT-116 stable cell lines. Confluent monolayer cells were scraped with sterile 200 µl pipette tip and allowed to migrate for 72 h. The wounded areas were photographed at 0 and 72 h. (**B**) Wound areas were calculated by Image J. Totally 18 wound areas in two wells of six-well plate of each cell line were calculated. Percentage of closure area = [(wound area at 0 h − wound area at 72 h)/wound area at 0 h] × 100%. $^{*}P < 0.05$, $^{***}P < 0.001$. (**C** and **D**) Transwell invasion assay of HCT-116 stable cell lines. 5×10^4 cells were allowed to invade the matrigel for 72 h. Invaded cells were fixed and stained with crystal violet. Representative pictures of invaded cells were shown in (C; scale bar, 50 µm).The invaded cells from five 100 × fields were counted under a phase-contrast microscope and statistical results were shown in (D).Results shown are mean ± standard deviation. $^{*}P < 0.05$, $^{***}P < 0.001$. (**E**) Representative immunostaining of endothelia cells in the indicated HCT-116 xenografts with an anti-CD31 antibody. (**F**) CD31-positive cells of the xenografts were counted in five high-power fields and averaged as the mean microvessel density, presenting the number of vessels per mm^2 calculated described in Materials and methods. Results are presented as mean ± standard deviation. $^{*}P < 0.05$, $^{***}P < 0.001$.

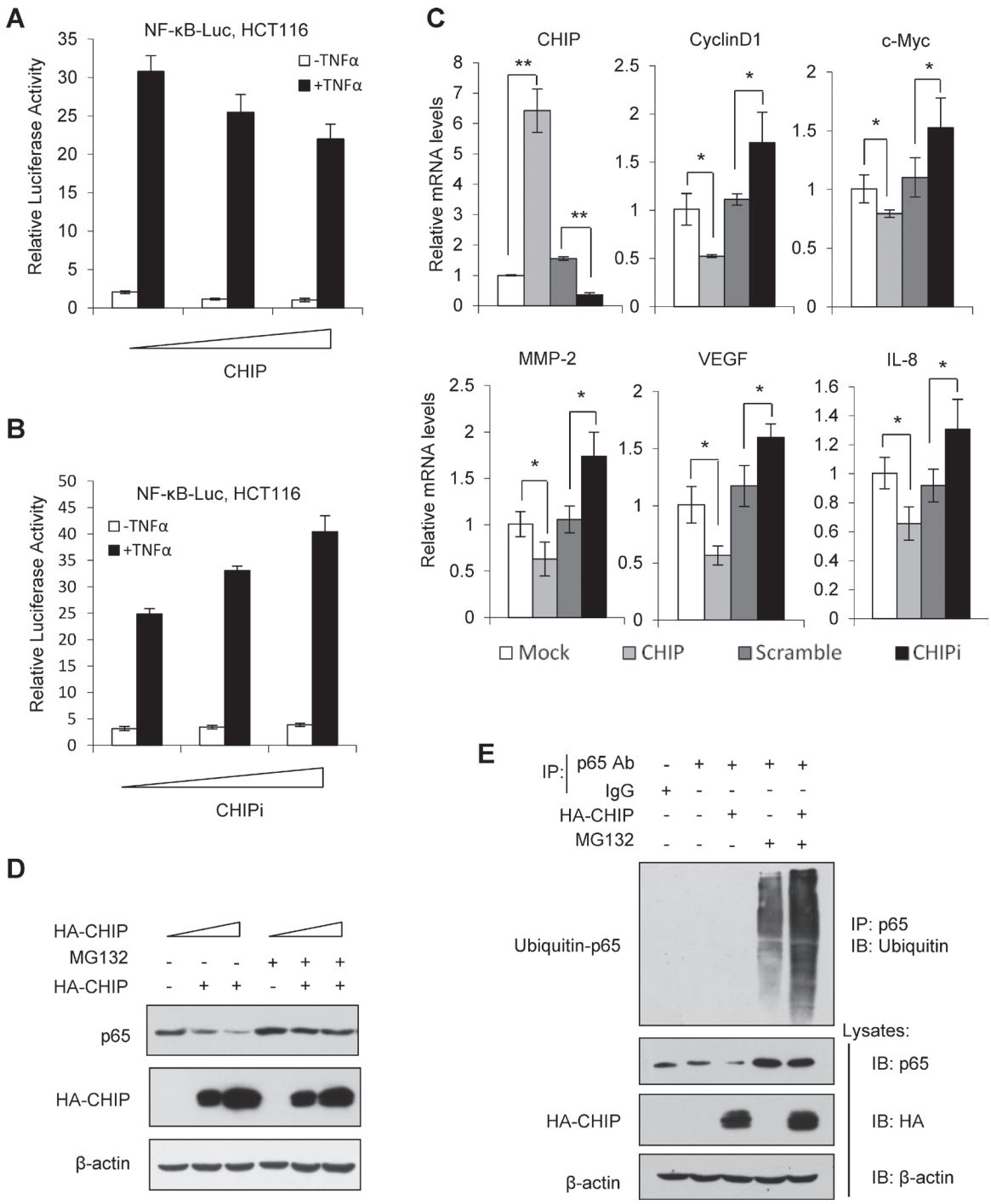

Fig. 5. CHIP negatively regulates NF-κB signaling by promoting degradation of p65. (**A** and **B**) CHIP inhibits NF-κB signaling. HCT-116 cells were cotransfected with pGL3-NF-κB-Luc, pRL-TK and an increased amount of pEFneo-HA CHIP (CHIP, A) or pSilencer-CHIP shRNA (CHIPi, B) plasmids. After serum starvation for overnight, cells were treated with or without tumor necrosis factor α (10 ng/ml) for 8 h. Results presented are from one experiment of triplicate. (**C**) Overexpression of CHIP downregulates, but depletion of CHIP upregulates, the NF-κB targeted genes. Messenger RNA expression (normalized to glyceraldehyde-3-phosphate dehydrogenase) of NF-κB target genes was analyzed by quantitative real-time PCR (qPCR). Results are presented as mean ± standard deviation. $*P < 0.05$, $**P < 0.01$. (**D**) CHIP mediates degradation of p65. HCT-116 cells were transfected with an increased amount of pEFneo-HA CHIP. Cells were treated with or without MG132 (10 μM) for 6 h before harvest. Cell lysates were subjected to western blot analyses with respective antibodies as shown. (**E**) CHIP promotes ubiquitination of p65. HCT-116 cells were transfected with pEFneo-HA CHIP or pEFneo-HA plasmid as a control. Cells were treated with or without MG132 (10 μM) for 6 h before harvest. Cell lysates were subjected to IP with anti-p65 antibody or rabbit immunoglobin G as a control followed by immunoblot with respective antibodies as shown. Smear bands showed the ubiquitinated p65 proteins.

CHIP has been reported to regulate the stability of several proteins including CFTR (5), GR (6) and mutant SOD1 (7). Our previous studies indicated that CHIP regulated the stability of Smads (8), Runx1 (9) and Runx2 (10) *in vitro*. Recently, CHIP has been reported to mediate degradation of several oncogenic proteins including ErbB2 (11), hypoxia inducible factor 1α (12), c-Myc (13), Runx1 (9), estrogen receptor α (14), Met receptor (15) and SRC-3 (16). In particular, it has been suggested that CHIP functions as a tumor suppressor and is downregulated in human breast cancer (16) and gastric cancer (17). It appeared that CHIP targeted SRC-3 (16), an important oncoprotein regulating tumor

cell proliferation, in breast cancers and NF-κB in gastric cancer (17). Our study supported that NF-κB is targeted by CHIP in CRC. However, we cannot exclude the probability that CHIP may also target other oncoproteins besides NF-κB in CRCs. High-throughput screening can be performed to identify CHIP targets in various human cancers to better understand the regulatory mechanisms of CHIP in tumor development.

In summary, we found that CHIP protein level was frequently decreased in colorectal cancer, associated with TNM stage. We reasoned that the decreased level of CHIP expression might be due to hypermethylation of the *CHIP* promoter. As strong evidence was provided for the role of CHIP in downregulation of NF-κB signaling by mediating degradation of p65, we proposed that downregulation of CHIP in the CRC facilitated the NF-κB signaling, which causes the enhanced tumor growth, migration, invasion and angiogenesis. It will be important to further examine both the prognostic significance of CHIP and to explore whether it may play a role in mediating tumor responsiveness to treatment and therefore be useful as a predictive marker. Further characterization of its role in critical tumor related pathways could present new opportunities for exploitation in novel treatment strategies.

Funding

The 973 Project (2011CB910502, 2006CB910102), the National Natural Science Foundation of China (81230044, 31071225, 30470888, 81228013), the 863 project (2012AA021703), the Ministry of Science and Technology of the People's Republic of China Project (2011ZX08011-006) in China, Tsinghua Internal Foundation (20091081322, 20111080996).

Conflict of Interest Statement: None declared.

References

1. Kerr,D. (2003) Clinical development of gene therapy for colorectal cancer. *Nat. Rev. Cancer*, **3**, 615–622.
2. Vogelstein,B. *et al*. (2013) Cancer genome landscapes. *Science*, **339**, 1546–1558.
3. Grivennikov,S. *et al*. (2009) IL-6 and Stat3 are required for survival of intestinal epithelial cells and development of colitis-associated cancer. *Cancer Cell*, **15**, 103–113.
4. Ballinger,C.A. *et al*. (1999) Identification of CHIP, a novel tetratricopeptide repeat-containing protein that interacts with heat shock proteins and negatively regulates chaperone functions. *Mol. Cell. Biol*., **19**, 4535–4545.
5. Meacham,G.C. *et al*. (2001) The Hsc70 co-chaperone CHIP targets immature CFTR for proteasomal degradation. *Nat. Cell Biol*., **3**, 100–105.
6. Connell,P. *et al*. (2001) The co-chaperone CHIP regulates protein triage decisions mediated by heat-shock proteins. *Nat. Cell Biol*., **3**, 93–96.
7. Urushitani,M. *et al*. (2004) CHIP promotes proteasomal degradation of familial ALS-linked mutant SOD1 by ubiquitinating Hsp/Hsc70. *J. Neurochem*., **90**, 231–244.
8. Li,L. *et al*. (2004) CHIP mediates degradation of Smad proteins and potentially regulates Smad-induced transcription. *Mol. Cell. Biol*., **24**, 856–864.
9. Shang,Y. *et al*. (2009) CHIP functions an E3 ubiquitin ligase of Runx1. *Biochem. Biophys. Res. Commun*., **386**, 242–246.
10. Li,X. *et al*. (2008) CHIP promotes Runx2 degradation and negatively regulates osteoblast differentiation. *J. Cell Biol*., **181**, 959–972.
11. Zhou,P. *et al*. (2003) ErbB2 degradation mediated by the co-chaperone protein CHIP. *J. Biol. Chem*., **278**, 13829–13837.
12. Bento,C.F., *et al*. (2010) The chaperone-dependent ubiquitin ligase CHIP targets HIF-1alpha for degradation in the presence of methylglyoxal. *PLoS One*, **5**, e15062.
13. Paul,I. *et al*. (2013) The ubiquitin ligase CHIP regulates c-Myc stability and transcriptional activity. *Oncogene*, **32**, 1284–1295.
14. Fan,M. *et al*. (2005) CHIP (carboxyl terminus of Hsc70-interacting protein) promotes basal and geldanamycin-induced degradation of estrogen receptor-alpha. *Mol. Endocrinol*., **19**, 2901–2914.
15. Jang,K.W. *et al*. (2011) The C-terminus of Hsp70-interacting protein promotes Met receptor degradation. *J. Thorac. Oncol*., **6**, 679–687.
16. Kajiro,M. *et al*. (2009) The ubiquitin ligase CHIP acts as an upstream regulator of oncogenic pathways. *Nat. Cell Biol*., **11**, 312–319.
17. Wang,S. *et al*. (2013) CHIP functions as a novel suppressor of tumour angiogenesis with prognostic significance in human gastric cancer. *Gut*, **62**, 496–508.
18. Wang,F. *et al*. (2008) Varp interacts with Rab38 and functions as its potential effector. *Biochem. Biophys. Res. Commun*., **372**, 162–167.
19. Su,F. *et al*. (2012) Protein tyrosine phosphatase Meg2 dephosphorylates signal transducer and activator of transcription 3 and suppresses tumor growth in breast cancer. *Breast Cancer Res*., **14**, R38.
20. Franken,N.A. *et al*. (2006) Clonogenic assay of cells *in vitro*. *Nat. Protoc*., **1**, 2315–2319.
21. Liang,C.C. *et al*. (2007) *In vitro* scratch assay: a convenient and inexpensive method for analysis of cell migration *in vitro*. *Nat. Protoc*., **2**, 329–333.
22. Huang,M.C. *et al*. (2006) C2GnT-M is downregulated in colorectal cancer and its re-expression causes growth inhibition of colon cancer cells. *Oncogene*, **25**, 3267–3276.
23. Sakamoto,K. *et al*. (2009) Constitutive NF-kappaB activation in colorectal carcinoma plays a key role in angiogenesis, promoting tumor growth. *Clin. Cancer Res*., **15**, 2248–2258.
24. Hatakeyama,S. (2011) TRIM proteins and cancer. *Nat. Rev. Cancer*, **11**, 792–804.
25. Welcker,M. *et al*. (2008) FBW7 ubiquitin ligase: a tumour suppressor at the crossroads of cell division, growth and differentiation. *Nat. Rev. Cancer*, **8**, 83–93.
26. Cheng,Y. *et al*. (2012) Role of the ubiquitin ligase Fbw7 in cancer progression. *Cancer Metastasis Rev*., **31**, 75–87.
27. Zhao,D. *et al*. (2010) The Fbw7 tumor suppressor targets KLF5 for ubiquitin-mediated degradation and suppresses breast cell proliferation. *Cancer Res*., **70**, 4728–4738.
28. Wu,W. *et al*. (2008) The ubiquitin E3 ligase activity of BRCA1 and its biological functions. *Cell Div*., **3**, 1.
29. Baer,R. *et al*. (2002) The BRCA1/BARD1 heterodimer, a tumor suppressor complex with ubiquitin E3 ligase activity. *Curr. Opin. Genet. Dev*., **12**, 86–91.
30. Khacho,M. *et al*. (2009) Subcellular dynamics of the VHL tumor suppressor: on the move for HIF degradation. *Future Oncol*., **5**, 85–95.
31. Haase,V.H. (2009) The VHL tumor suppressor: master regulator of HIF. *Curr. Pharm. Des*., **15**, 3895–3903.
32. Chen,B.B. *et al*. (2012) F-box protein FBXL2 targets cyclin D2 for ubiquitination and degradation to inhibit leukemic cell proliferation. *Blood*, **119**, 3132–3141.
33. Chen,B.B. *et al*. (2012) F-box protein FBXL2 exerts human lung tumor suppressor-like activity by ubiquitin-mediated degradation of cyclin D3 resulting in cell cycle arrest. *Oncogene*, **31**, 2566–2579.
34. Pei,X.H. *et al*. (2011) Cytoplasmic CUL9/PARC ubiquitin ligase is a tumor suppressor and promotes p53-dependent apoptosis. *Cancer Res*., **71**, 2969–2977.
35. Hanahan,D. *et al*. (2011) Hallmarks of cancer: the next generation. *Cell*, **144**, 646–674.
36. Sakamoto,K. *et al*. (2010) Targeting NF-kappaB for colorectal cancer. *Expert Opin. Ther. Targets*, **14**, 593–601.

Received April, 12, 2013; revised October 9, 2013; accepted November 8, 2013